Letter

Dynamics of active polar ring polymers

Christian A. Philipps [1,2,*] Gerhard Gompper [1,†] and Roland G. Winkler [1,‡]

[1]*Theoretical Physics of Living Matter, Institute of Biological Information Processing and Institute for Advanced Simulation, Forschungszentrum Jülich and JARA, 52425 Jülich, Germany*

[2]*Department of Physics, RWTH Aachen University, 52056 Aachen, Germany*

(Received 31 January 2022; revised 17 March 2022; accepted 23 May 2022; published 15 June 2022)

The conformational and dynamical properties of isolated semiflexible active polar ring polymers are investigated analytically. A ring is modeled as a continuous Gaussian polymer exposed to tangential active forces. The analytical solution of the linear non-Hermitian equation of motion in terms of an eigenfunction expansion shows that ring conformations are independent of activity. In contrast, activity strongly affects the internal ring dynamics and yields characteristic time regimes, which are absent in passive rings. On intermediate timescales, flexible rings show an activity-enhanced diffusive regime, while semiflexible rings exhibit ballistic motion. Moreover, a second active time regime emerges on longer timescales, where rings display a snake-like motion, which is reminiscent to a tank-treading rotational dynamics in shear flow, dominated by the mode with the longest relaxation time.

DOI: 10.1103/PhysRevE.105.L062501

I. INTRODUCTION

Filaments and polymers are fundamental ingredients of living matter and essential for the diverse functions of eukaryotic and prokaryotic cells. The out-of-equilibrium processes in these cells affect the conformations and dynamics of the immanent polymeric structures. Molecular motors walking along microtubule filaments generate forces that determine the dynamics of the cytoskeletal network and the organization of the cell interior [1–4]. Even more, molecular motors give rise to nonequilibrium conformational fluctuations of actin filaments and microtubules [5,6]. Within the nucleus, ATPases such as DNA or RNA polymerase (DNAP and RNAP, respectively) are involved in DNA transcription and every RNAP or DNAP translocation step generates nonthermal fluctuations for both RNAP and DNAP and the transcribed DNA [7–10]. Among the wide spectrum of polymeric structures, chromosomes in bacteria [11], archaea, chloroplasts, and even mitochondrial [12] and extrachromosomal DNA [13] of eukaryote cells are of a circular nature, similarly, actomyosin aggregates in cytokinesis and marginal bands formed by microtubules in blood cells [14–16]. The circular shape substantially affects their dynamical behavior which deviates from that of comparable linear structures. This is emphasized in experiments on microtubules placed on motility assays, which reveal ringlike structures [17–19] and an emergent rotational motion [17,19].

The desire to unravel the underlying physical phenomena and to gain insight into the emergent behaviors of the out-of-equilibrium polymeric structures has prompted intensive studies on tangentially (active polar) [4,10,20–28] and isotropically (active Brownian) [10,29–40] driven or self-propelled linear filaments and polymers—so-called active polymers. Even experiments on living worms as a model system resembling tangentially driven polymers have been performed [41]. These studies reveal a strong influence of the active forces on the polymer conformations and dynamics, and can lead to polymer swelling [29,31,35] or shrinkage [24–27,38], depending on the kind of active force and the environment [10,24,25,37,39].

Active polymers are typically studied by computer simulations employing various discrete models [10], which differ in the way the tangential forces are applied, yet yield the same continuum limit for smooth contours [25–27]. However, a severe problem arises for flexible discrete polymers, where the bending angles are not restricted and can become very large, which renders the definition of a tangent vector arbitrary—related to the well-known property of random walks to generate nondifferentiable trajectories. Moreover, analytical descriptions and results, which could serve as a guide to uncover model-specific discretization phenomena, for active polar ring polymers (APRPs) are lacking [28].

To address this fundamental question, we present analytical results for the conformations and dynamics of continuous phantom semiflexible APRPs, based on a Gaussian polymer model [42,43]. Due to the activity, the equation of motion is non-Hermitian and the solution in terms of an eigenfunction representation yields complex eigenvalues. The latter imply a particular internal ring dynamics, distinctly different from that of passive rings, with a snakelike motion along their contour for all stiffnesses, which is similar to a tank-treading rotational motion known for passive ring polymers [44,45] and vesicles [46,47] under shear flow. Hence, we denote this dynamical behavior as *active tank-treading*. This is reflected in characteristic time regimes, with an enhanced diffusive and a ballistic dynamics for flexible and semiflexible rings,

*c.philipps@fz-juelich.de
†g.gompper@fz-juelich.de
‡r.winkler@fz-juelich.de

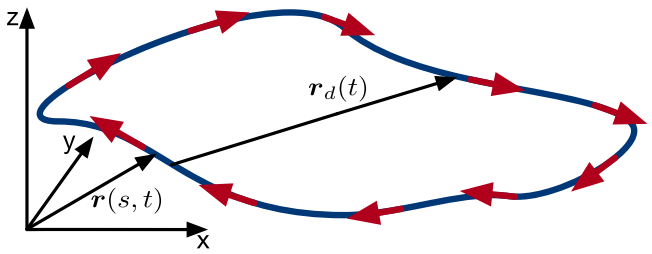

FIG. 1. Illustration of an active polar ring polymer. The arrows indicate the local tangential active force. An arbitrary position vector $\boldsymbol{r}(s,t)$ and the ring diameter vector $\boldsymbol{r}_d(t)$ are shown.

respectively. We find marked qualitative and quantitative differences to the results of previous simulations of a discrete model [27], like an average ring size, which is found to be independent of activity in our model, but has been predicted to display a very strong swelling in Ref. [27]. We also present results of a modified discrete model [24], which yields qualitative agreement with our continuum predictions.

II. MODEL

The ring polymer is described as a continuous, differentiable space curve $\boldsymbol{r}(s,t)$ embedded in three dimensions, where $s \in [0, L)$ is the contour variable along the ring and t the time (Fig. 1). We adopt the Gaussian semiflexible polymer model [42,43], which yields the overdamped—the inertia term is omitted—equation of motion for an APRP,

$$\gamma \frac{\partial \boldsymbol{r}(s,t)}{\partial t} = 2k_BT\lambda \frac{\partial^2 \boldsymbol{r}(s,t)}{\partial s^2} - k_BT\epsilon \frac{\partial^4 \boldsymbol{r}(s,t)}{\partial s^4} + \boldsymbol{\Gamma}(s,t) + f_a \frac{\partial \boldsymbol{r}(s,t)}{\partial s}, \tag{1}$$

where γ is the translational friction coefficient per length, k_B the Boltzmann constant, and T the temperature (cf. Supplemental Material [48]). The bending rigidity is given by $\epsilon = 3/(4p)$, with $p = 1/(2l_p)$, in terms of the persistence length l_p. The Lagrangian multiplier λ is determined by the inextensibility of the ring contour via the local constraint of the mean-square tangent vector $\langle(\partial \boldsymbol{r}(s,t)/\partial s)^2\rangle = 1$ [35,40]. The homogeneous external or internal active force of magnitude f_a acts in the direction of the local tangent $\partial \boldsymbol{r}(s,t)/\partial s$. Thermal fluctuations are captured by the stochastic force $\boldsymbol{\Gamma}(s,t)$, which is assumed to be stationary, Markovian, and Gaussian with zero mean and second moment $\langle \boldsymbol{\Gamma}(s,t) \cdot \boldsymbol{\Gamma}(s',t')\rangle = 6\gamma k_BT\delta(s-s')\delta(t-t')$.

The linear, but non-Hermitian, Langevin equation (1) is solved by the eigenfunction expansion $\boldsymbol{r}(s,t) = \sum_{m=-\infty}^{\infty} \boldsymbol{\chi}_m(t)\phi_m(s)$ with the eigenfunctions $\phi_m(s) = e^{ik_m s}/\sqrt{L}$ and the wave numbers $k_m = 2\pi m/L$, which satisfy the periodic boundary condition $\boldsymbol{r}(s,t) = \boldsymbol{r}(s+L,t)$ by the ring structure. Insertion of the expansion into Eq. (1) yields the equations of motion for the normal-mode amplitudes, $\boldsymbol{\chi}_m(t)$,

$$\gamma \frac{d}{dt}\boldsymbol{\chi}_m(t) = -\xi_m \boldsymbol{\chi}_m(t) + \boldsymbol{\Gamma}_m(t). \tag{2}$$

The eigenvalues ξ_m of the eigenvalue problem are given by ($m \in \mathbb{Z}$)

$$\xi_m = \frac{12\pi^2 k_BT\,pL}{L^3}\left[\frac{\pi^2}{(pL)^2}m^4 + \mu m^2 - i\frac{\mathrm{Pe}}{6\pi\,pL}m\right], \tag{3}$$

with the abbreviation $\mu = 2\lambda/(3p)$ and the Péclet number

$$\mathrm{Pe} = \frac{f_aL^2}{k_BT}, \tag{4}$$

which characterizes the strength of the activity. The ξ_m are complex due to the non-Hermitian nature of the underlying equation with the first-order derivative, which implies a dynamical behavior absent in passive systems and active polar linear polymers. The correlation functions of the normal-mode amplitudes determine the ring dynamics and capture the influence of the activity. Explicitly, they are given in the stationary state by ($m \neq 0$)

$$\langle \boldsymbol{\chi}_m(t) \cdot \boldsymbol{\chi}_n^*(t')\rangle = \delta_{mn}\frac{3k_BT}{\gamma}\tau_m e^{-|t-t'|/\tau_m}e^{i\omega_m|t-t'|}, \tag{5}$$

where $\boldsymbol{\chi}_m^*(t) = \boldsymbol{\chi}_{-m}(t)$. Here, the eigenvalues $\xi_m = \xi_m^R - i\xi_m^I$ are separated in real and imaginary parts, and the relaxation times $\tau_m = \gamma/\xi_m^R$ and frequencies $\omega_m = \xi_m^I/\gamma = 2\pi f_a m/(\gamma L)$ are introduced, where τ_m is activity independent and identical with the relaxation time of a passive ring [40]. Most importantly, the non-Hermitian nature of a ring's equation of motion implies complex correlation functions with an activity-dependent frequency. Note that at equal times $t = t'$, the active contribution in Eq. (5) vanishes and $\langle \boldsymbol{\chi}_m(t) \cdot \boldsymbol{\chi}_n^*(t)\rangle$ is equal to the equilibrium correlation function of a passive ring. This illustrates that tangential active propulsion of a continuous polymer only impacts the ring dynamics but not its conformations.

III. DYNAMICS

The translational motion of a ring is characterized by its mean-square displacement (MSD), $\langle \Delta \boldsymbol{r}_{\mathrm{tot}}^2(t)\rangle = \langle(\boldsymbol{r}(s,t) - \boldsymbol{r}(s,0))^2\rangle$, which can be separated into a contribution from the center-of-mass motion, $\langle \Delta \boldsymbol{r}_{\mathrm{cm}}^2(t)\rangle$, and a ring internal part, $\langle \Delta \boldsymbol{r}^2(t)\rangle$, such that $\langle \Delta \boldsymbol{r}_{\mathrm{tot}}^2(t)\rangle = \langle \Delta \boldsymbol{r}_{\mathrm{cm}}^2(t)\rangle + \langle \Delta \boldsymbol{r}^2(t)\rangle$. Due to the ring structure, the MSD is independent of the contour variable s. Moreover, by integrating the Langevin equation (1) over the ring contour, all internal and active forces vanish, and the center-of-mass diffusion is solely determined by thermal fluctuations with the diffusion coefficient $D_0 = k_BT/(\gamma L)$ of a passive ring. This is at variance to the model applied in Ref. [27], where the sum of active forces along the ring polymer is nonzero. On the contrary, in tangentially driven active polar linear polymers, the sum over the active forces must obviously be large, and an activity-enhanced long-time diffusion coefficient is obtained [24,25,28].

The MSD in the center-of-mass reference frame is given by

$$\langle \Delta \boldsymbol{r}^2(t)\rangle = \frac{12k_BT}{\gamma L}\sum_{m=1}^{\infty}\tau_m(1 - \cos(\omega_m t)e^{-t/\tau_m}). \tag{6}$$

Compared to a passive ring, with $\mathrm{Pe} = 0$ (4), an additional periodic function, $\cos(\omega_m t)$, appears for active rings, which determines the MSD over certain timescales $t/\tau_1 \lesssim 1$, where

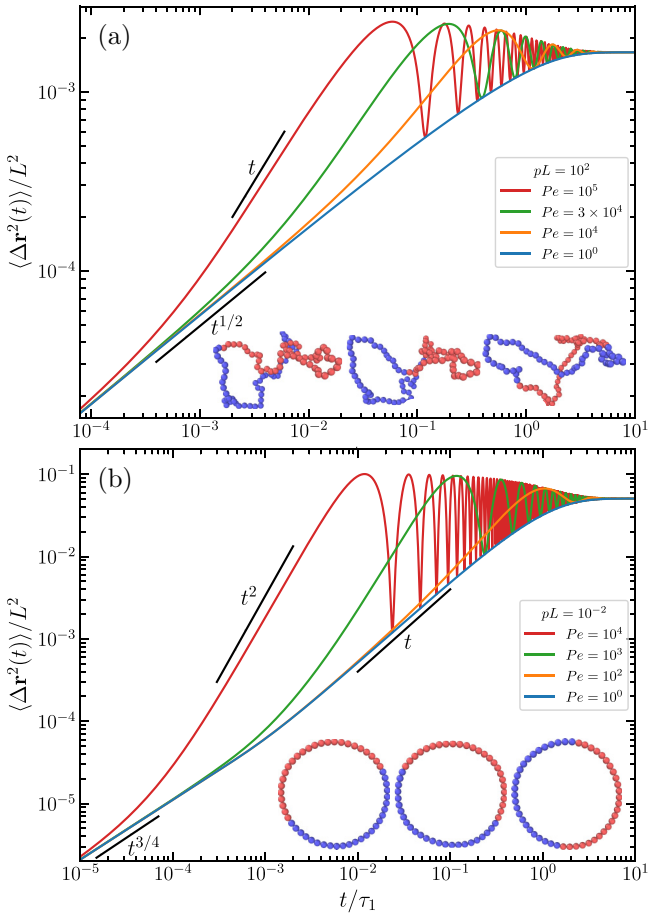

FIG. 2. Normalized mean-square displacement in the center-of-mass reference frame, $\langle \Delta \boldsymbol{r}^2(t) \rangle$, of (a) flexible, $pL = 10^2$, and (b) semiflexible, $pL = 10^{-2}$, APRPs as function of the time t/τ_1, where τ_1 is the longest relaxation time, for various Péclet numbers Pe (increasing from bottom to top). The black lines show power laws with the indicated time dependence. The insets show subsequent conformations with $\Delta t \approx 1/\omega_1$ of discrete flexible and semiflexible polymers of length $L = 50l$. To illustrate the clockwise reptation motion, half of the monomers are colored blue and red, respectively.

τ_1 is the longest relaxation time. Equation (6) reveals two relevant timescales, the longest polymer relaxation time τ_1, and the oscillation period by the lowest frequency ω_1. With the relaxation time $\tau_1 = \gamma L^3/(12\pi^2 k_B T pL)$ of flexible and $\tau_1 = \gamma L^3/(24\pi^2 k_B T)$ of semiflexible rings [40], the relation

$$\omega_1 \tau_1 \approx \begin{cases} \dfrac{\mathrm{Pe}}{6\pi\, pL}, & pL \gg 1 \\ \dfrac{\mathrm{Pe}}{12\pi}, & pL \ll 1 \end{cases} \tag{7}$$

is obtained, which determines the importance of the cosine term.

Figure 2 displays MSDs of flexible and semiflexible APRPs for various Péclet numbers. As shown in Fig. 2(a), on timescales $t/\tau_1 \ll 1/(\omega_1\tau_1)^2 \ll 1$, flexible polymers exhibit the well-known subdiffusive time dependence $t^{1/2}$ predicted by the Rouse model [49,50]. In the range $1/(\omega_1\tau_1)^2 < t/\tau_1 \ll 1/(\omega_1\tau_1)$, an activity-enhanced linear time regime appears for $\mathrm{Pe} \gtrsim 10^4$, where

$$\langle \Delta \boldsymbol{r}^2(t) \rangle \approx \frac{L^2}{12\pi^2} \frac{\mathrm{Pe}}{(pL)^2} \frac{t}{\tau_1}, \tag{8}$$

with a linear Pe dependence. For longer times, $1/(\omega_1\tau_1) < t/\tau_1 \lesssim 1$, oscillations due to the cosine term emerge. Here, all modes contribute to the MSD [48].

Figure 2(b) for semiflexible polymers reveals a qualitatively similar behavior, with the characteristic time dependence $t^{3/4}$ [51,52] for $t/\tau_1 \ll \min\{pL, (pL)^{1/5}/(\omega_1\tau_1)^{8/5}\}$. In the range of $(pL)^{1/5}/(\omega_1\tau_1)^{8/5} < t/\tau_1 \ll 1/(\omega_1\tau_1)$, the MSD is dominated by the first mode, which yields $\langle \Delta \boldsymbol{r}^2(t) \rangle \sim t$ for $\mathrm{Pe} \ll 1$ [48,52], whereas for large Péclet numbers the active ballistic time regime

$$\left\langle \Delta \boldsymbol{r}^2(t) \right\rangle \approx \frac{L^2 \mathrm{Pe}^2}{576\pi^4} \left(\frac{t}{\tau_1} \right)^2 \tag{9}$$

emerges [48]. Here, the MSD shows a quadratic dependence on the Péclet number and is independent of persistence length. At times $t/\tau_1 \gtrsim 1/(\omega_1\tau_1)$, $\langle \Delta \boldsymbol{r}^2(t) \rangle$ is well described by

$$\left\langle \Delta \boldsymbol{r}^2(t) \right\rangle \approx \frac{L^2}{2\pi^2} (1 - \cos(\omega_1 t) e^{-t/\tau_1}), \tag{10}$$

and oscillations appear.

The difference in the Pe dependence between flexible and semiflexible APRPs reflects the underlying distinctive conformations. Flexible polymers are coiled and all modes contribute to the internal dynamics. In contrast, semiflexible APRPs assume circular conformations and their dynamics on timescales $t/\tau_1 > 1/(\omega_1\tau_1)$ is described by the mode with the longest relaxation time corresponding to a rotational motion.

The oscillations appear as long as $\omega_1\tau_1 > 1$, i.e., the polymer relaxation time is longer than the period by the frequency ω_1. This is reflected in Fig. 2, which illustrates that the oscillations disappear with decreasing Pe. Notice that the polymer relaxation time is independent of Pe, but ω_1 is, which stresses the active nature of the effect.

To characterize the oscillations in the ring polymer dynamics, the temporal autocorrelation function of the ring diameter vector $\boldsymbol{r}_d(t) = \boldsymbol{r}(L/2, t) - \boldsymbol{r}(0, t)$ is considered (Fig. 1). Analytically, its correlation function is given by

$$\langle \boldsymbol{r}_d(t) \cdot \boldsymbol{r}_d(0) \rangle = \frac{24 k_B T}{\gamma L} \sum_{\substack{m=1 \\ m \text{ odd}}}^{\infty} \tau_m \cos(\omega_m t)\, e^{-t/\tau_m}. \tag{11}$$

The cosine term yields significant contributions as long as $\omega_1\tau_1 > 1$ on timescales $t/\tau_1 \lesssim 1$. As shown in Eq. (7), the product $\omega_1\tau_1$ increases linearly with increasing Pe for any stiffness, hence, oscillations always appear for sufficiently large Péclet numbers. Note that $\omega_1\tau_1$ for $pL \ll 1$ is independent of ring stiffness and length. This yields a universal dynamical behavior in terms of $\omega_1\tau_1$ for $t/\tau_1 < 1$. For flexible polymers, $\omega_1\tau_1$ depends on pL, and the Péclet number has to exceed the value of $6\pi\, pL$ to observe oscillations, which requires much larger Péclet numbers compared to semiflexible rings. As shown in Fig. 3, for $\mathrm{Pe} = 10^3$ the correlation function already decays exponentially for $pL \gtrsim 50$.

In the regime of pronounced oscillations, the correlation function for all ring stiffnesses is determined by the first mode

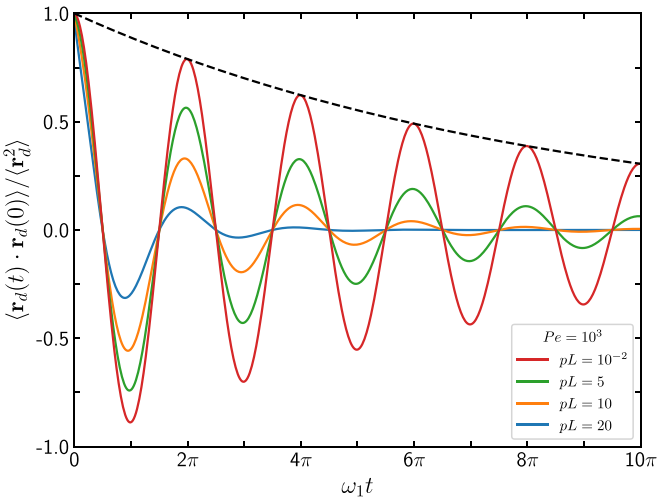

FIG. 3. Normalized autocorrelation function of the ring diameter $\boldsymbol{r}_d(t)$ as a function of the time $\omega_1 t$, where $\omega_1 = 2\pi f_a/(\gamma L)$, for $\mathrm{Pe} = 10^3$ and various pL values as indicated in the legend (increasing from bottom to top at $\omega_1 t = \pi$). The dashed line corresponds to the exponential $\exp(-t/\tau_1) = \exp(-12\pi\omega_1 t/\mathrm{Pe})$. Curves for $pL < 10^{-2}$ are indistinguishable from that with $pL = 10^{-2}$.

in Eq. (11), i.e.,

$$\frac{\langle \boldsymbol{r}_d(t) \cdot \boldsymbol{r}_d(0) \rangle}{\langle \boldsymbol{r}_d^2 \rangle} \approx C_\omega \cos(\omega_1 t) e^{-t/\tau_1}, \tag{12}$$

with the equilibrium mean-square diameter $\langle \boldsymbol{r}_d^2 \rangle$ [40,48] of the passive ring and a stiffness-dependent constant C_ω. In the case of a flexible polymer, the amplitude is $C_\omega = 8/\pi^2$, and its deviation from unity reflects the influence of higher modes. In fact, the deviation is below 20% for all pL values. The ring performs an active tank-treading motion along the slowly varying instantaneous conformation when $\mathrm{Pe} > 6\pi\, pL$, with the frequency ω_1, corresponding to the tangential velocity f_a/γ (cf. Supplemental Material, movies M1 and M2 [48]).

The correlation function of semiflexible rings, $pL < 1$, is governed by the first mode only and the longest relaxation time is independent of pL, hence, $C_\omega = 1$. The damped periodic dynamics corresponding to a tank-treading rotation of the ring with the frequency ω_1 (cf. Supplemental Material, movie M3 [48]). In general, activity implies a tank-treading motion and the thermal (passive) contributions control the damping.

IV. DISCUSSION

Our analytical studies of continuous semiflexible APRPs reveal substantial differences compared to simulations of rings modeled by discrete points, which is related to the definition of the active force. In Ref. [27], the tangential force $\tilde{\boldsymbol{F}}_i = F_a \boldsymbol{t}_i$, with the unit vector $\boldsymbol{t}_i = (\boldsymbol{r}_{i+1} - \boldsymbol{r}_{i-1})/|\boldsymbol{r}_{i+1} - \boldsymbol{r}_{i-1}|$ and strength F_a, on particle i is applied, where $\boldsymbol{r}_{i\pm1}$ are the positions of the neighboring particles along the ring contour. For any discrete ring, this active force differs from the alternative discretization $\boldsymbol{F}_i = F_a(\boldsymbol{r}_{i+1} - \boldsymbol{r}_{i-1})/(2l)$, with the bond length $|\boldsymbol{r}_{i+1} - \boldsymbol{r}_i| = l$, which is the sum of the forces $\boldsymbol{F}_i = F_a(\boldsymbol{R}_{i+1} + \boldsymbol{R}_i)/(2l)$ along the two bond vectors, where $\boldsymbol{R}_i = \boldsymbol{r}_i - \boldsymbol{r}_{i-1}$ (cf. Supplemental Material [48]) [24]. As the angle between two subsequent bonds changes, $\boldsymbol{F}_i$ varies strongly—it assumes a maximum for parallel and vanishes for antiparallel bond alignment. In contrast, the force $\tilde{\boldsymbol{F}}_i$ is independent of the angle between the successive bonds. In both cases, the force is tangential to the contour, and turns into the active force in Eq. (1) in the continuum limit.

Most importantly, the conformations of the continuous rings are independent of activity. This is in stark contrast to simulations based on the tangential force $\tilde{\boldsymbol{F}}_i$ [27], which predict a strong swelling of phantom polymers with increasing activity by approximately 250% of the mean radius-of-gyration at the Péclet number $\mathrm{Pe} = F_a l/(k_B T) = 10$ (cf. Supplemental Material of Ref. [27]). We have performed Brownian dynamics simulations of flexible and semiflexible APRPs applying the active forces $\boldsymbol{F}_i$ to resolve the fundamental difference in the ring conformations (cf. Ref. [48]). These simulations for flexible rings, with $\mathrm{Pe} = 20$, yield a small shrinkage of the ring by approximately 10% of the root mean-square radius-of-gyration with respect to its value at equilibrium. This constitutes a very minor conformational change compared to that observed in Ref. [27] and is consistent with our analytical results. The discrepancy reveals a strong influence of the discretization of the active force on the ring conformations. In addition, the integral over the active force in Eq. (1) is zero, i.e., a ring's center-of-mass dynamics is independent of the active force. Again, this is in contrast to simulations applying the active force of Ref. [27].

Experimental realizations of synthetic active rings using self-propelled Janus particles show variations in the Janus-particle orientations, and their propulsion directions are not always necessarily tangential [53]. However, biological filaments such as microtubules, actin filaments, and circular chromosomes need to be described by a semiflexible polymer model, at least on a local scale, and the difference between the various discretization schemes is expected to be of minor importance. We expect our theoretical approach to capture the essential features of such APRPs.

The discussed dynamical properties of APRPs should be experimentally accessible via structures formed by microtubules [16,18,19] or actin filaments driven by molecular motors. For a microtubule of length $L = 1\,\mu$m, the force per motor $F_a = 6\,$pN, and $N = 10$ active motors, the Péclet number at room temperature is $\mathrm{Pe} = N F L/(k_B T) \approx 10^4$ [54], on the order of the Péclet numbers in Figs. 2 and 3. Experiments on microtubules placed on motility assays indeed exhibit rotational motion [17,19], consistent with our prediction. A tank-treading motion can also be expected for circular aggregates of crosslinked microtubules [16] or actin filaments. Such structures can be synthesized and would provide, in combination with motility assays, insight into the nonequilibrium dynamical properties of flexible and semiflexible APRPs.

We have focused on the dynamical properties of idealized active rings. Passive rings in a melt exhibit strong conformational changes and shrinkage with increasing concentration [55,56]. Here, excluded-volume interactions with and entanglements by the surrounding polymers play a major role. It

is not *a priori* evident how the conformations of active rings are affected in this case. However, the predicted active tank-treading dynamics will certainly be present.

ACKNOWLEDGMENTS

We would like to thank J. Midya and G. A. Vliegenthart for constructive discussions.

[1] A. W. C. Lau, B. D. Hoffmann, A. Davies, J. C. Crocker, and T. C. Lubensky, Microrheology, Stress Fluctuations, and Active Behavior of Living Cells, Phys. Rev. Lett. **91**, 198101 (2003).

[2] F. C. MacKintosh and A. J. Levine, Nonequilibrium Mechanics and Dynamics of Motor-Activated Gels, Phys. Rev. Lett. **100**, 018104 (2008).

[3] W. Lu, M. Winding, M. Lakonishok, J. Wildonger, and V. I. Gelfand, Microtubule–microtubule sliding by kinesin-1 is essential for normal cytoplasmic streaming in Drosophila oocytes, Proc. Natl. Acad. Sci. USA **113**, E4995 (2016).

[4] A. Ravichandran, G. A. Vliegenthart, G. Saggiorato, T. Auth, and G. Gompper, Enhanced dynamics of confined cytoskeletal filaments driven by asymmetric motors, Biophys. J. **113**, 1121 (2017).

[5] C. P. Brangwynne, G. H. Koenderink, F. C. MacKintosh, and D. A. Weitz, Cytoplasmic diffusion: Molecular motors mix it up, J. Cell Biol. **183**, 583 (2008).

[6] C. A. Weber, R. Suzuki, V. Schaller, I. S. Aranson, A. R. Bausch, and E. Frey, Random bursts determine dynamics of active filaments, Proc. Natl. Acad. Sci. USA **112**, 10703 (2015).

[7] M. Guthold, X. Zhu, C. Rivetti, G. Yang, N. H. Thomson, S. Kasas, H. G. Hansma, B. Smith, P. K. Hansma, and C. Bustamante, Direct observation of one-dimensional diffusion and transcription by Escherichia coli RNA polymerase, Biophys. J. **77**, 2284 (1999).

[8] Y. X. Mejia, E. Nudler, and C. Bustamante, Trigger loop folding determines transcription rate of *Escherichiacoli's* RNA polymerase, Proc. Natl. Acad. Sci. USA **112**, 743 (2015).

[9] V. Belitsky and G. M. Schütz, Stationary RNA polymerase fluctuations during transcription elongation, Phys. Rev. E **99**, 012405 (2019).

[10] R. G. Winkler and G. Gompper, The physics of active polymers and filaments, J. Chem. Phys. **153**, 040901 (2020).

[11] F. Wu, A. Japaridze, X. Zheng, J. Wiktor, J. W. J. Kerssemakers, and C. Dekker, Direct imaging of the circular chromosome in a live bacterium, Nat. Commun. **10**, 2194 (2019).

[12] R. P. Koche, E. Rodriguez-Fos, K. Helmsauer, M. Burkert, I. C. MacArthur, J. Maag, R. Chamorro, N. Munoz-Perez, M. Puiggròs, H. Dorado Garcia, Y. Bei, C. Röefzaad, V. Bardinet, A. Szymansky, A. Winkler, T. Thole, N. Timme, K. Kasack, S. Fuchs, F. Klironomos *et al.*, Extrachromosomal circular DNA drives oncogenic genome remodeling in neuroblastoma, Nat. Genet. **52**, 29 (2020).

[13] X. Cao, S. Wang, L. Ge, W. Zhang, J. Huang, and W. Sun, Extrachromosomal circular DNA: Category, biogenesis, recognition, and functions, Front. Vet. Sci. **8**, 976 (2021).

[14] I. M. Sehring, P. Recho, E. Denker, M. Kourakis, B. Mathiesen, E. Hannezo, B. Dong, and D. Jiang, Assembly and positioning of actomyosin rings by contractility and planar cell polarity, Elife **4**, e09206 (2015).

[15] T. H. Cheffings, N. J. Burroughs, and M. K. Balasubramanian, Actomyosin ring formation and tension generation in eukaryotic cytokinesis, Curr. Biol. **26**, R719 (2016).

[16] S. Dmitrieff, A. Alsina, A. Mathur, and F. J. Nédélec, Balance of microtubule stiffness and cortical tension determines the size of blood cells with marginal band across species, Proc. Natl. Acad. Sci. USA **114**, 4418 (2017).

[17] R. Kawamura, A. Kakugo, K. Shikinaka, Y. Osada, and J. P. Gong, Ring-shaped assembly of microtubules shows preferential counterclockwise motion, Biomacromolecules **9**, 2277 (2008).

[18] L. Liu, E. Tüzel, and J. L. Ross, Loop formation of microtubules during gliding at high density, J. Phys.: Condens. Matter **23**, 374104 (2011).

[19] J. J. Keya, A. M. R. Kabir, and A. Kakugo, Synchronous operation of biomolecular engines, Biophys. Rev. **12**, 401 (2020).

[20] F. Peruani, A. Deutsch, and M. Bär, Nonequilibrium clustering of self-propelled rods, Phys. Rev. E **74**, 030904(R) (2006).

[21] M. Abkenar, K. Marx, T. Auth, and G. Gompper, Collective behavior of penetrable self-propelled rods in two dimensions, Phys. Rev. E **88**, 062314 (2013).

[22] M. Bär, R. Großmann, S. Heidenreich, and F. Peruani, Self-propelled rods: Insights and perspectives for active matter, Annu. Rev. Condens. Matter Phys. **11**, 441 (2020).

[23] T. B. Liverpool, A. C. Maggs, and A. Ajdari, Viscoelasticity of Solutions of Motile Polymers, Phys. Rev. Lett. **86**, 4171 (2001).

[24] R. E. Isele-Holder, J. Elgeti, and G. Gompper, Self-propelled worm-like filaments: Spontaneous spiral formation, structure, and dynamics, Soft Matter **11**, 7181 (2015).

[25] V. Bianco, E. Locatelli, and P. Malgaretti, Globulelike Conformation and Enhanced Diffusion of Active Polymers, Phys. Rev. Lett. **121**, 217802 (2018).

[26] S. K. Anand and S. P. Singh, Structure and dynamics of a self-propelled semiflexible filament, Phys. Rev. E **98**, 042501 (2018).

[27] E. Locatelli, V. Bianco, and P. Malgaretti, Activity-Induced Collapse and Arrest of Active Polymer Rings, Phys. Rev. Lett. **126**, 097801 (2021).

[28] M. S. E. Peterson, M. F. Hagan, and A. Baskaran, Statistical properties of a tangentially driven active filament, J. Stat. Mech. (2020) 013216.

[29] A. Ghosh and N. S. Gov, Dynamics of active semiflexible polymers, Biophys. J. **107**, 1065 (2014).

[30] J. Harder, C. Valeriani, and A. Cacciuto, Activity-induced collapse and reexpansion of rigid polymers, Phys. Rev. E **90**, 062312 (2014).

[31] A. Kaiser and H. Löwen, Unusual swelling of a polymer in a bacterial bath, J. Chem. Phys. **141**, 044903 (2014).

[32] A. Kaiser, S. Babel, B. ten Hagen, C. von Ferber, and H. Löwen, How does a flexible chain of active particles swell? J. Chem. Phys. **142**, 124905 (2015).

[33] S. Chaki and R. Chakrabarti, Enhanced diffusion, swelling, and slow reconfiguration of a single chain in non-Gaussian active bath, J. Chem. Phys. **150**, 094902 (2019).

[34] J. Shin, A. G. Cherstvy, W. K. Kim, and R. Metzler, Facilitation of polymer looping and giant polymer diffusivity in crowded solutions of active particles, New J. Phys. **17**, 113008 (2015).

[35] T. Eisenstecken, G. Gompper, and R. G. Winkler, Conformational properties of active semiflexible polymers, Polymers **8**, 304 (2016).

[36] T. Eisenstecken, G. Gompper, and R. G. Winkler, Internal dynamics of semiflexible polymers with active noise, J. Chem. Phys. **146**, 154903 (2017).

[37] A. Martín-Gómez, T. Eisenstecken, G. Gompper, and R. G. Winkler, Active Brownian filaments with hydrodynamic interactions: Conformations and dynamics, Soft Matter **15**, 3957 (2019).

[38] S. K. Anand and S. P. Singh, Conformation and dynamics of a self-avoiding active flexible polymer, Phys. Rev. E **101**, 030501(R) (2020).

[39] A. Martin-Gomez, T. Eisenstecken, G. Gompper, and R. G. Winkler, Hydrodynamics of polymers in an active bath, Phys. Rev. E **101**, 052612 (2020).

[40] S. M. Mousavi, G. Gompper, and R. G. Winkler, Active Brownian ring polymers, J. Chem. Phys. **150**, 064913 (2019).

[41] A. Deblais, A. C. Maggs, D. Bonn, and S. Woutersen, Phase Separation by Entanglement of Active Polymerlike Worms, Phys. Rev. Lett. **124**, 208006 (2020).

[42] R. G. Winkler, Deformation of semiflexible chains, J. Chem. Phys. **118**, 2919 (2003).

[43] L. Harnau, R. G. Winkler, and P. Reineker, Dynamic properties of molecular chains with variable stiffness, J. Chem. Phys. **102**, 7750 (1995).

[44] W. Chen, J. Chen, and L. An, Tumbling and tank-treading dynamics of individual ring polymers in shear flow, Soft Matter **9**, 4312 (2013).

[45] M. Liebetreu, M. Ripoll, and C. N. Likos, Trefoil knot hydrodynamic delocalization on sheared ring polymers, ACS Macro Lett. **7**, 447 (2018).

[46] S. R. Keller and R. Skalak, Motion of a tank-treading ellipsoidal particle in a shear flow, J. Fluid Mech. **120**, 27 (1982).

[47] H. Noguchi and G. Gompper, Fluid Vesicles with Viscous Membranes in Shear Flow, Phys. Rev. Lett. **93**, 258102 (2004)

[48] See Supplemental Material at http://link.aps.org/supplemental/10.1103/PhysRevE.105.L062501 for details of the model and derivations, including Ref. [57], and movies of Brownian dynamics simulations.

[49] M. Doi and S. F. Edwards, *The Theory of Polymer Dynamics* (Clarendon Press, Oxford, 1986)

[50] K. Hur, R. G. Winkler, and D. Y. Yoon, Comparison of ring and linear polyethylene from molecular dynamics simulations, Macromolecules **39**, 3975 (2006).

[51] E. Farge and A. C. Maggs, Dynamic scattering from semiflexible polymers, Macromolecules **26**, 5041 (1993).

[52] R. G. Winkler, Diffusion and segmental dynamics of rodlike molecules by fluorescence correlation spectroscopy, J. Chem. Phys. **127**, 054904 (2007).

[53] D. Nishiguchi, J. Iwasawa, H.-R. Jiang, and M. Sano, Flagellar dynamics of chains of active janus particles fueled by an AC electric field, New J. Phys. **20**, 015002 (2018).

[54] B. Rupp and F. Nédélec, Patterns of molecular motors that guide and sort filaments, Lab Chip **12**, 4903 (2012).

[55] M. Kapnistos, M. Lang, D. Vlassopoulos, W. Pyckhout-Hintzen, D. Richter, D. Cho, T. Chang, and M. Rubinstein, Unexpected power-law stress relaxation of entangled ring polymers, Nat. Mater. **7**, 997 (2008).

[56] S. Y. Reigh and D. Y. Yoon, Concentration dependence of ring polymer conformations from Monte Carlo simulations, ACS Macro Lett. **2**, 296 (2013).

[57] M. Bixon and R. Zwanzig, Optimized Rouse–Zimm theory for stiff polymers, J. Chem. Phys. **68**, 1896 (1978).